

Measurements of strongly localized potential well profiles in an inertial electrostatic fusion neutron source

K. Yoshikawa^a, K. Takiyama^b, T. Koyama^a, K. Taruya^a,
K. Masuda^a, Y. Yamamoto^a, T. Toku^a, T. Kii^a, H. Hashimoto^a,
N. Inoue^a, M. Ohnishi^c, H. Horiike^d

^a Institute of Advanced Energy, Kyoto University, Uji, Kyoto

^b Hiroshima University, Higashi, Hiroshima

^c Kansai University, Suita, Osaka

^d Osaka University, Suita, Osaka

Japan

Abstract. Direct measurements of localized electric fields have been made by the laser induced fluorescence (LIF) method using the Stark effect in the central cathode core region of an inertial electrostatic confinement fusion (IECF) neutron (proton) source. These are expected to have various applications, such as luggage security inspection, non-destructive testing, land mine detection and positron emitter production for cancer detection, currently producing continuously about 10^7 n/s D–D neutrons. Since 1967, when the first fusion reaction was successfully proved to have taken place in a very compact IECF device, potential well formation due to the space charge associated with spherically converging ion beams has been a central key issue remaining to be clarified in beam–beam collision fusion, which is the major mechanism of the IECF neutron source. Many experiments, although indirect, have been done so far to clarify the nature of the potential well, but none of them has produced definitive evidence. The results found by the present LIF method show a double well potential profile with a slight dip for ion beams with relatively larger angular momenta, whereas for ions with smaller angular momenta, a much steeper potential peak develops.

1. Introduction

Potential well formation due to the space charge associated with spherically converging ion beams plays a key role in beam–beam collision fusion, which is the major mechanism of inertial electrostatic confinement fusion (IECF) devices. At present, D–D fusion neutrons at rates of several millions per second are being successfully produced continuously at several institutions [1].

Many theoretical results so far have predicted strongly localized potential well formation and, over the past 30 years, many experiments have been dedicated to clarifying this mechanism using, for example, the electron beam reflection method [2], spatially collimated neutron profile [3] or proton profile [1, 4] measurements and emissive probes [5], but, none can provide definitive evidence [1].

Recently some theoretical predictions [6] have called for a higher degree of time and spatial resolution of the diagnostics, which have not been achieved by the conventional methods used so far.

After an elaborate survey, we decided to adopt optical diagnostics by using Stark effects, which are sensitive to local electric fields [7]. In addition, to enhance the S/N ratio as well as to specify the radial potential profile, we have introduced the laser induced fluorescence (LIF) method [7, 8]. Detailed examination of the application of the LIF method to IECF has revealed that:

- (a) A wavelength resolution of about 0.4 nm is required.
- (b) A spatial resolution of 1 mm^3 requires a 2^1S He atom density of more than 10^{10} cm^{-3} .

In addition, a Nd:YAG laser pumped dye laser was set up for the diagnostics of the potential well of our IECF device. Very recently preliminary measurements have been made with the LIF method and show a double well potential profile for the first time in a He plasma [8]. Since the theoretical predictions indicate significant effects of the angular momentum of the spherically converging ion beams on the potential profiles, they are investigated in this study [9].

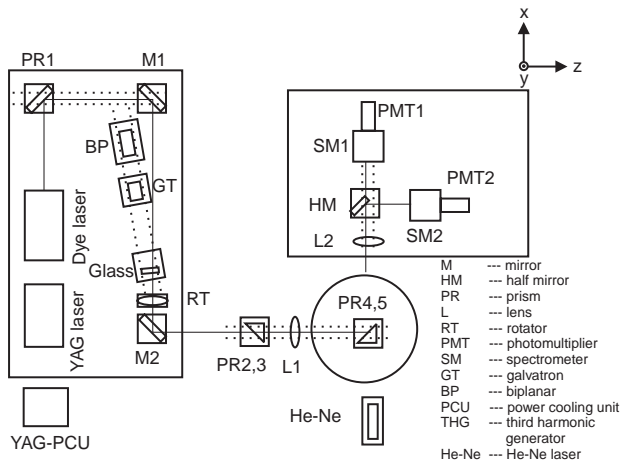


Figure 1. Experimental set-up for LIF diagnostics.



Figure 2. A hollow cathode made of tantalum in an IECF device. The vacuum chamber has an inner diameter of 340 mm and the Ta cathode grid has an inner diameter of 50 mm, an outer diameter of 60 mm and a thickness of 0.3 mm.

2. Experimental set-up

The LIF system consists of a Nd:YAG laser (continuum Surelite II-10-JST; 355 nm, 160 mJ) and a dye laser (continuum ND6000; linewidth 0.07–0.08 cm^{-1} at 515 and 560 nm) with two spectrometers (Jobin Yvon TR190MS2; dispersion $<4 \text{ nm/mm}$). A polarization rotator is fitted between the dye laser and the IECF injection quartz window, and a polarization plate is fitted between the IECF window and the spectroscop to measure the effects of polarization, as shown in Fig. 1.

We have chosen in the experiments an IECF device with a hollow cathode, with the IECF device being spherical and made of SS304 steel with an inner diameter of 34 cm, while the hollow cathode of 5 cm inner diameter, held at the centre by the insulator, is made of 5 mm wide curved Ta sheets of 0.3 mm thickness, which were precisely cut by a laser (Fig. 2).

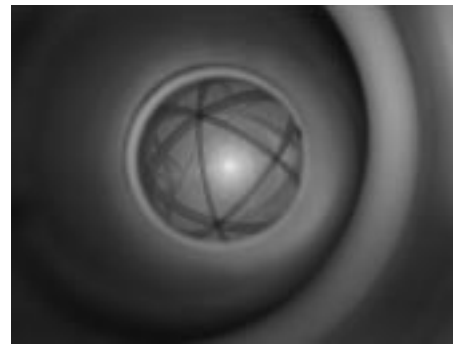


Figure 3. The IECF plasma core at the centre of the hollow cathode taken from the laser exit (in the y direction).

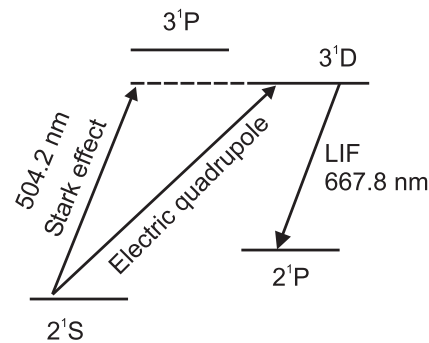


Figure 4. Relevant energy diagram for the LIF process of He I in an electric field.

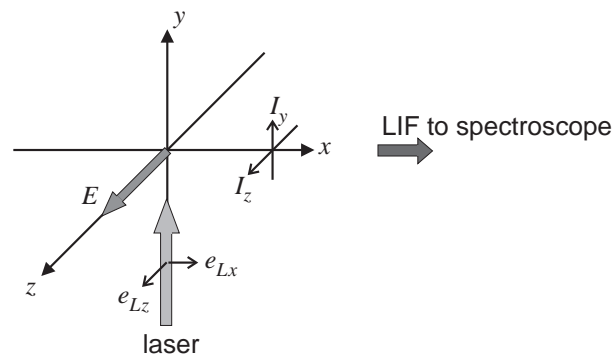


Figure 5. Observation geometry for LIF.

The laser wavelength was precisely calibrated within 1 pm through optogalvanic effects by a galva-tron (GT in Fig. 1). To measure the spatial profile, a laser beam injected in the y direction was scanned horizontally in the z direction (vertically in Fig. 3). A He gas was chosen, and the metastable atoms (2^1S) were excited to 3^1D by the laser (504.2 nm) with two different polarizations (e_{Lx} , e_{Lz}) through forbidden transitions, i.e. the Stark induced electric dipole

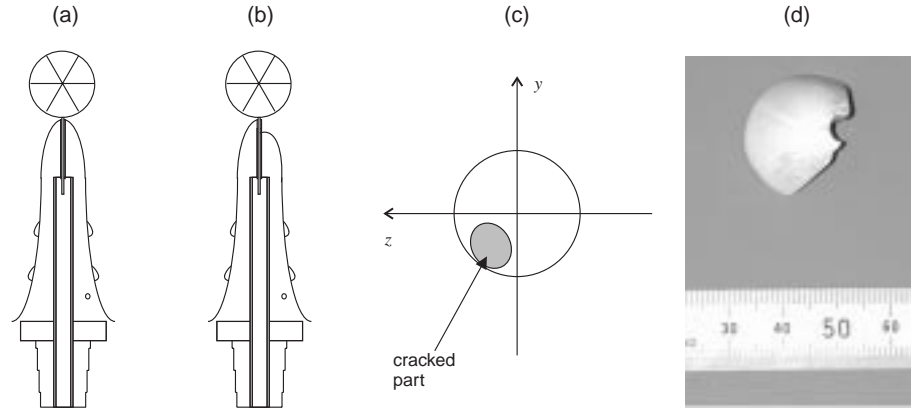


Figure 6. Insulator (Macerite) shapes: (a) original (normal), (b) cracked. Cracked part of insulator: (c) position, (d) photograph of same.

moment, and electric quadrupole (QDP) moment transitions (Fig. 4) [10].

3. Method of polarized laser induced fluorescence for measurements of local electric fields

Use of the fact that the fluorescence polarization (667.8 nm; 3^1D-2^1P) due to Stark excitation is quite different from that due to QDP excitation thus makes it possible to evaluate the local electric field by measuring four kinds of polarized radiation ($I_z(\mathbf{e}_{Lz})$, $I_y(\mathbf{e}_{Lz})$, $I_z(\mathbf{e}_{Lx})$, $I_y(\mathbf{e}_{Lx})$) in terms of the degree of polarization (Fig. 5) [10]. LIF (667.8 nm) is then observed along the x axis. Both the polarized components I_z and I_y are detected. The degree of polarization is defined by

$$P = \frac{I_z - I_y}{I_z + I_y}. \quad (1)$$

In the experiments, a He pressure of 31 mtorr, a cathode voltage of 7.5 kV and a cathode current of 40 mA were typically chosen to enhance beam perveance. Two kinds of operation were studied with respect to the ion beams with relatively larger and smaller angular momenta, which were provided by the shape of the cathode insulators, i.e. asymmetric and symmetric, respectively, as is seen in Fig. 6 with theoretical potential profiles (Fig. 7) for the normal insulator of Fig. 6(a).

Although the insulator, made of Macerite (basically made of mica and ceramics with an approximate dielectric constant of 6), was manufactured to have the original shape shown in Fig. 6(a), during the discharge experiments part of the top was

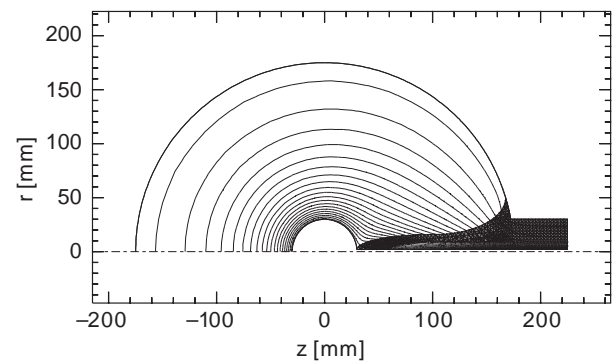


Figure 7. Potential distribution for a normal insulator (only the upper half is shown).

cracked due most probably to frequent breakdown, as is shown in Figs 6(c, d). This was expected to eventually cause asymmetrically converging ion beams, i.e. beams with enhanced angular momenta. We could thus have made measurements of both cases, i.e. under the conditions of the cracked shape and complete insulator shape cases for comparison.

According to theoretical predictions, double well potential profiles with depressed potential peaks are expected to develop for the former case, while for the latter case a relatively steep potential profile would result [9].

Helium metastable atoms (2^1S) are excited to a given magnetic sublevel in 3^1D by the laser through forbidden transitions, i.e. Stark induced electric dipole moment and electric QDP moment transitions, as shown in Fig. 4 [10].

According to the alignment of atoms achieved with the polarized laser excitation and the selection rules for the relevant radiative transition between sublevels in the upper and lower states, electric fields

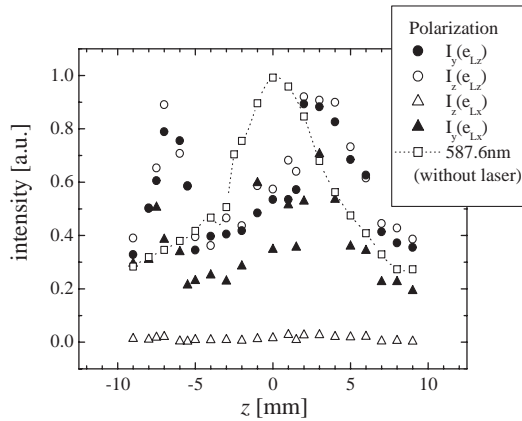


Figure 8. Profiles of four polarized components.

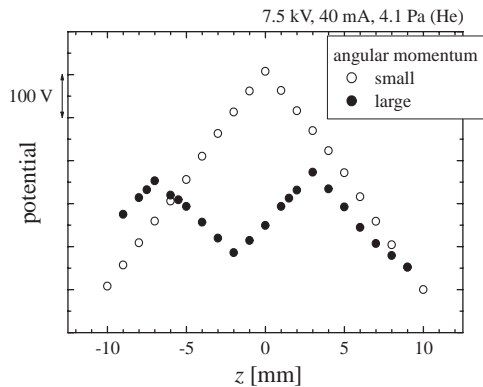


Figure 9. Potential profiles for ions with relatively larger (solid circles) and smaller (open circles) angular momenta.

E can be related to P [10] by the following relation:

$$E = C^x \sqrt{\frac{2(P+1)}{1-3P}} \quad (2)$$

where $C^x = 1.96$ kV/cm for the e_{Lx} excitation. Integration over E thus yields potential profiles.

4. Results and discussion

Spatial profiles of LIF peak intensity are plotted in Fig. 8 for ions with enhanced angular momenta together with the intensity profile of the radiation at 587.6 nm, which corresponds to the visible image. Profiles of three polarization components, $I_z(e_{Lz})$, $I_y(e_{Lz})$ and $I_y(e_{Lx})$ are considered as approximately the profiles of collisionally excited He metastable atoms (2^1S), which are sensitive to electron temperature in the range $T_e \leq 20$ eV. The peaks are thus thought to correspond to the potential peaks where electrons with ample energies are expected to exist.

On the other hand, the intensity of $I_z(e_{Lx})$ is due to the Stark effect, with which electric fields can be evaluated together with $I_y(e_{Lx})$ on the basis of Eqs (1) and (2). The potential profiles for the two cases thus obtained are shown in Fig. 9. It is clearly seen that a double well potential forms for ion beams with larger angular momenta, but that for ions with smaller angular momenta the potential has only one peak that is much steeper compared with the double well potential, and this is consistent with theoretical predictions [9].

Intentional production of ion beams with specific angular momenta will need to be explored for further detailed experiments on the potential well profiles.

Acknowledgements

We would like to thank Y. Nishinosono for manufacturing various parts of the experimental equipment, and we are grateful to JAERI for supporting this study through the Nuclear Research Promotion Program (JANP).

References

- [1] Miley, G.H., et al., in Current Trends in International Fusion Research (Proc. 2nd Symp. Ottawa, 1999), NRCC, Ottawa (1999) 177.
- [2] Swanson, D.A., et al., Phys. Fluids **16** (1973) 1939.
- [3] Hirsh, R.L., J. Appl. Phys. **38** (1967) 4522.
- [4] Thorson, T.A., et al., Nucl. Fusion **38** (1998) 495.
- [5] Thorson, T.A., et al., Phys. Plasmas **4** (1997) 4.
- [6] Ohnishi, M., et al., Nucl. Fusion **37** (1997) 611.
- [7] Takiyama, K., et al., Jpn. J. Appl. Phys. **25** (1986) L455.
- [8] Yoshikawa, K., et al., in Fusion Energy (Proc. 18th Symp. Albuquerque, 2000) 27.
- [9] Matsuura, H., "Ion distribution function and radial profile of neutron production rate in spherical inertial electrostatic confinement plasmas", paper presented at US-Japan Workshop on IEC Neutron Sources, 2000.
- [10] Takiyama, K., et al., in Laser Aided Plasma Diagnostics (Proc. 6th Int. Symp. Bar Harbor, 1993) 43.

(Manuscript received 4 October 2000

Final manuscript accepted 5 February 2001)

E-mail address of K. Yoshikawa:
kiyoshi@iae.kyoto-u.ac.jp

Subject classification: K0, Ie